REGULAR PAPER

Multi Junction Solar Cells Stacked with Transparent and Conductive Adhesive

Toshiyuki Sameshima[1*], Jun Takenezawa[1], Masahiko Hasumi[1], Takashi Koida[2],
Tetsuya Kaneko[2], Minoru Karasawa[2], and Michio Kondo[2]

[1]*Tokyo University of Agriculture and Technology, 2-24-16, Naka-cho, Koganei, Tokyo 184-8588, Japan*
[2]*National Institute of Advanced Industrial Science and Technology, Tsukuba, Ibaraki 305-8568, Japan*

We propose a polyimide transparent adhesive layer dispersed with In_2O_3–SnO_2 (ITO) conductive particles (polyimide-ITO) to be used in the mechanical stacking of solar cells. A 20-μm-thick polyimide-ITO layer had a high transmissivity from 78 to 80% for wavelengths ranging from 500 to 1000 nm and a low connecting resistivity of $2.3\,\Omega\,cm^2$ at minimum. The fabrication of stacked cell consisting of a top hydrogenated amorphous silicon (a-Si:H) p–i–n cell and a bottom hetero-junction with an intrinsic thin-layer (HIT)-type silicon cell was demonstrated using an intermediate polyimide-ITO layer. A high open circuit voltage of 1.34 V was experimentally obtained. Simultaneous electric power generation from the top and bottom solar cells was achieved. © 2011 The Japan Society of Applied Physics

1. Introduction

Semiconductor solar cells have been widely investigated as a device for generating electrical power directly from sunlight.[1,2] Multijunction solar cells with different band gaps are attractive for effectively collecting sunlight, which has a wide-range spectrum from ultraviolet to infrared.[3,4] Growth technologies of multiple semiconductor layers with different band gaps have therefore been developed.[5–10] They have resulted in demonstrations of multijunction solar cells with high open circuit voltages (V_{oc}).

We have proposed multijunction solar cells with different band gaps, which are fabricated by stacking individual solar cells used by intermediate adhesive layers, as shown by a structural image in Fig. 1.[11] Top cells and bottom cells are individually fabricated first. They are then combined as stacked cells using the adhesive. This strategy may have the advantage of high yield in cell fabrication because it allows the selection of good cells before the stacking process. Moreover, soft and low-temperature adhesion makes it possible to stack fragile or no-heat resistant materials. Many kinds of solar cells will therefoere be applied. It is natural that top and bottom cells should have far different spectral absorption characteristics for effectively collecting sunlight. In general, both cells have a photoabsorbance for photon energy higher than their band gap. The efficiency of power generation for a solar cell decreases as the photon energy increases above the band gap because V_{oc} is limited by the band gap. Therefore, it is better for top and bottom cells to have far different band gaps from each other to maintain their original efficiencies. To achieve the situation described above, the intermediate layer should be transparent to light passing through the top solar cell in order to illuminate the narrow-band-gap bottom solar cell. In addition, the intermediate layer must be electrically conductive to produce electrical current from the two cells. V_{oc} increases and becomes the sum of that of each cell when the both cells work well with light illumination. Moreover, the effective short circuit current density (J_{sc}) is limited by the lower value of J_{sc} for individual cells because the differential resistivity of solar cells is very high in the low-voltage region so that J_{sc} remains almost the same value upon additional voltage application caused by the other
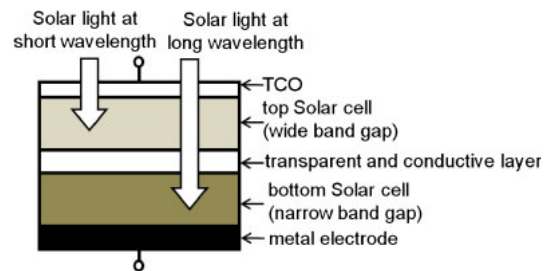

Fig. 1. (Color online) Structural image of a multijunction solar cell fabricated by stacking individual solar cells with intermediate adhesive layer.

cells. Proper selection of top and bottom cells with similar current density characteristis is therefore effective for stacked cells. The total resistance increases to the sum of the internal resistances of the individual cells and the connecting resistance of the intermediate adhesive. The additional resistance of the intermediate adhesive may therefore worsen solar cell characteristics, particularly fill factor (FF) and efficiency. If the connecting resistivity (R_c) is higher than the internal resistances of the individual cells and also much lower than V_{oc}/J_{sc}, FF is roughly given as

$$FF \sim FF_0 - \frac{R_c \times J_{sc}}{V_{oc}}, \qquad (1)$$

where FF_0 is the ideal value in the case of zero connecting resistivity. Although FF decreases as the connecting resistivity increases, the increase in V_{oc} as a result of stacking cells reduces the degree of FF. This will be one advantage of stacking cell technology.

In this paper, we discuss the optical and electrical connecting conditions of the inermediate adhesive layer. We propose a polyimide transparent adhesive layer dispersed with In_2O_3–SnO_2 (ITO) conductive particles. We report transmittance characteristics in visible and near-infrared wavelength ranges and the electrical conductance of the adhesive layers. Finally, we experimentally demonstrate multijunction solar cells by stacking an hydrogenated amorphous silicon (a-Si:H) p–i–n thin film solar cell on a heterojunction with an intrinsic thin-layer (HIT)-type silicon solar cells. We show an increase in V_{oc} owing to the multijunction effect.

*E-mail address: tsamesim@cc.tuat.ac.jp

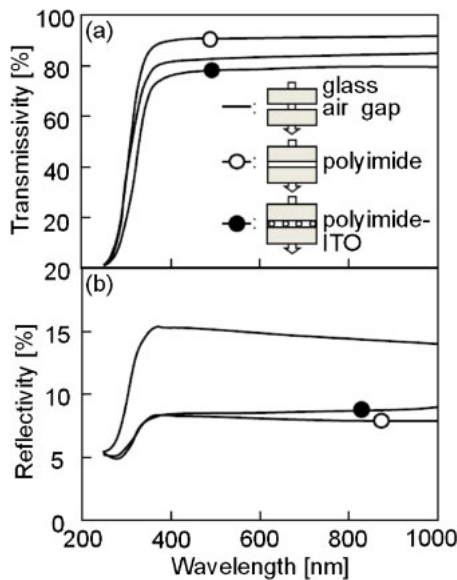© 2011 The Japan Society of Applied Physics

Fig. 2. (Color online) Optical transmissivity (a) and reflectivity spectra (b) for samples of a 20-μm-thick polyimide layer sandwiched by glass substrates, a 20-μm-thick polyimide layer dispersed with ITO particles sandwiched by glass substrates, and two glass substrates placed separately.
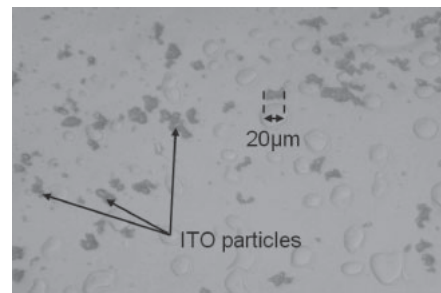

Fig. 3. Optical microscope image of polyimide-ITO layer formed on a glass substrate.

Fig. 4. Electrical current density as a function of voltage applied to a sample of doped-silicon/polyimide-ITO layer/doped-silicon with an area of 1 cm^2.

2. Intermediate Adhesive

We have investigated many organic binders to find candidates with a good transparent property. We selected transparent polyimide because it has been widely used in silicon technology as a stable intermediate layer. Figure 2 shows the optical transmissivity (a) and reflectivity spectra (b) of a 20-μm-thick polyimide layer sandwiched by glass substrates. Polyimide liquid was first spin-coated on a glass substrate. An another glass substrate was placed on the polyimide surface. The thickness of the polyimide was set to be about 20 μm using a spacer. The samples were heated at 150 °C for 2 h under a stress of 0.5 kg/cm^2 by placing a weight on the top glass substrate in order to solidify the polyimide layer with good adhesion. The sample had a good transmissivity of 91% in visible and near-infrared regions. The transmissivity was higher than that for two glass substrates placed separately. On the other hand, the reflectivity ranged from 8.2 to 7.9% between 500 and 1000 nm. The reflectivity was much lower than that for two glass substrates placed separately. The high transmissivity and low reflectivity results from index matching, since polyimide has a refractive index similar to that of glass so that there was low reflection loss at the air/glass interface.

As transparent conductive particles, we used commercial ITO particles with an average diameter of 20 μm and an average resistivity of 0.6 Ω cm. The resistivity of ITO was estimated by the measurement of the electrical conductance of a pellet made of ITO particles. ITO particles were mechanically dispersed in polyimide liquid by hand. The volume of ITO particles was set to be 0.05 g/cm^3 of polyimide liquid. Polyimide liquid including ITO particles (polyimide-ITO) was coated onto substrates using a spinner. A top substrate was placed on the polyimide-ITO layer, and then the polyimide-ITO layer was subsequently solidified by heating the samples at 150 °C for 2 h under a stress of

0.5 kg/cm^2. The thickness of the polyimide-ITO layers was about 20 μm, which was probably governed by ITO particles. Figure 3 shows the optical microscope image of the polyimide-ITO layer when glass substrates were used. ITO particles were randomly dispersed in polyimide. There was no serious condensation of ITO particles. The area ratio occupied by ITO particles was about 10%. The optical transmissivity and reflectivity of the sample, which consisted of glass/polyimide-ITO layer/glass, ranged from 78 to 80% and from 8.5 to 9.4%, respectively, for wavelength ranging from 500 to 1000 nm, as shown in Fig. 2. The polyimide-ITO layer was transparent over the wide range of visible and near infrared wavelengths. The transmissivity was lower by about 10% and reflectivity was slightly higher by about 1% than those for the sample of glass/polyimide/glass. We believe that those changes were mainly caused by optical scattering at polyimide/ITO interfaces. However, a small increase in the reflectivity indicates that high reflection caused by the high refractive index of ITO partially contributed the decrease in transmissivity.

Doped silicon substrates with a resistivity of 0.01 Ω cm were also used for investigating the electrical conductive property of the polyimide-ITO layer. Figure 4 shows th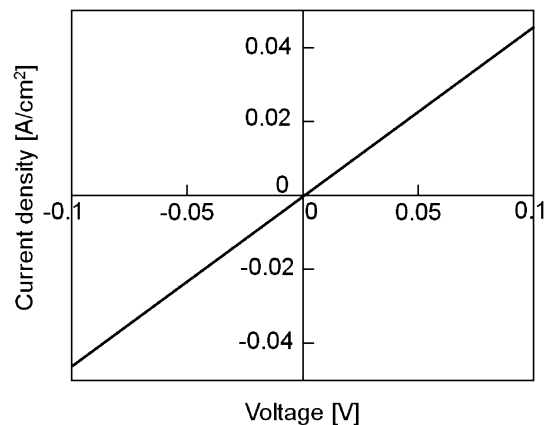e electrical current density as a function of voltage applied to a sample of doped-silicon/polyimide-ITO layer/doped-silicon with an area of 1 cm^2. A high electrical current density of 0.043 A/cm^2 was obtained upon the application of 0.1 V.

This means that the connecting resistivity of the intermediate polyimide-ITO layer was $2.3\,\Omega\,\mathrm{cm}^2$. The connecting resistivity depends on the amount of ITO particles. A good ohmic characteristic was achieved, as shown in Fig. 4. The lowest connecting resistivity was achieved by ITO particles 0.05 $\mathrm{g/cm}^3$ of polyimide liquid at present. The connecting resistivity increased as the amount of ITO particles decreased from 0.05 g. It also increased as the amount of ITO particles increased from 0.05 g, probably because the uniform dispersion of ITO was poor and condensation of ITO particles occurred. The connecting resistivity was distributed from 2.3 to $6\,\Omega\,\mathrm{cm}^2$ under the condition of ITO particles $0.05\,\mathrm{g/cm}^3$ of polyimide liquid. The connecting resistivity R_c is roughly given as

$$R_c = \frac{r \times d}{\eta \times A}, \qquad (2)$$

where η is the effective contact ratio of ITO particles to the silicon substrates, r is the average resistivity of ITO particles, d is the thickness of the intermediate layer, and A is the area ratio occupied by ITO particles. The ideally lowest R_c would be $0.012\,\Omega\,\mathrm{cm}^2$ under the present conditions of r of $0.6\,\Omega\,\mathrm{cm}$, d of 0.002 cm, and A of 0.1 if η were 1. The ideal R_c is much lower than the experimental R_c. This means that ITO particles were not in perfect contact with the top and bottom substrates. The η was estimated to be 0.005 at most. The low η probably results from variation in the size of ITO particles and their shapes. The development of conductive particles of a uniform size and a flat shape is important for increasing η and reducing R_c.

3. Stacked Solar Cells

In order to experimentally demonstrate multijunction stacked solar cells were fabricated by pasting a-Si:H p–i–n cells with an area of $1.08\,\mathrm{cm}^2$ onto HIT-type silicon solar cells with an area of $0.58\,\mathrm{cm}^2$, using the polyimide-ITO intermediate adhesive, as shown in Fig. 5(a). a-Si:H p–i–n cells were formed on glass substrates coated with a textured SnO_2 layer. p-, i-, and n-type a-Si:H layers were subsequently formed by plasma-enhanced chemical vapor deposition (PECVD). Finally, an ITO layer was coated onto the n-type a-Si:H surface. HIT-type silicon solar cells were fabricated in n-type crystalline silicon substrates by forming i- and p-type a-Si:H thin films using PECVD. The ITO layer was finally coated on the p-type a-Si:H surface. An air mass 1.5 (AM 1.5)-type solar simulator at $100\,\mathrm{mW/cm}^2$ was used for the measurement solar cell characteristics. Table I shows J_{sc}, V_{oc}, FF, and conversion efficiency for an a-Si:H p–i–n cell and a HIT-type cell. The a-Si:H p–i–n cell had a high V_{oc} of 0.86 V, and a low short circuit current (I_{sc}) and J_{sc} of $1.23 \times 10^{-2}\,\mathrm{A}$ and $1.14 \times 10^{-2}\,\mathrm{A/cm}^2$, respectively. The effective conversion efficiency was 7.49%. On the other hand, the HIT-type cell had a low V_{oc} of 0.58 V, and high I_{sc} and J_{sc} of $1.86 \times 10^{-2}\,\mathrm{A}$ and $3.2 \times 10^{-2}\,\mathrm{A/cm}^2$, respectively. The effective conversion efficiency was 14.4%. Table I also shows solar cell characteristics of the HIT-type cell when it was illuminated via the a-Si:H p–i–n cell as a filter. Because a-Si:H p–i–n cells have been not optimized to be the top cell, their transmissivity ranged from 45 to 55% for wavelengths between 700 and 1000 nm, as shown in Fig. 5(b). The a-Si:H p–i–n cell shaded the underlying HIT-
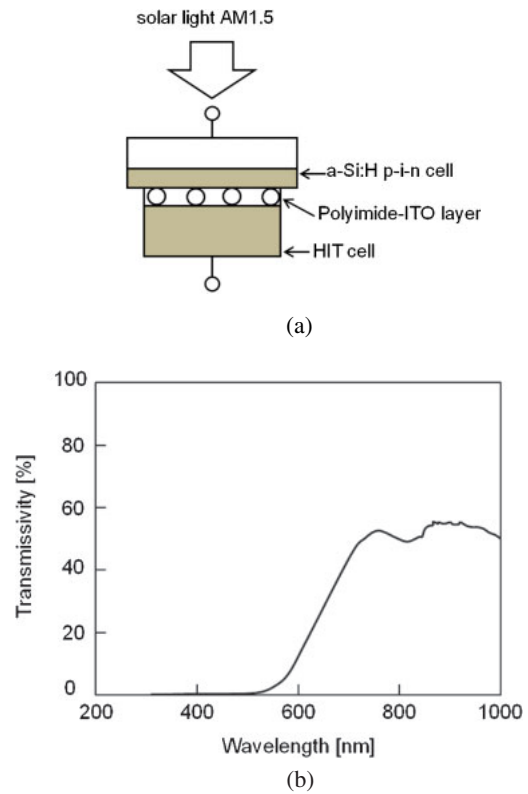

Fig. 5. (Color online) Schematic cross section of stacked cells with a top a-Si:H p–i–n cell with an area of $1.08\,\mathrm{cm}^2$ and a bottom HIT-type silicon solar cell with an area of $0.58\,\mathrm{cm}^2$ and with a polyimide-ITO intermediate adhesive (a) and transmissivity spectrum of the top a-Si:H p–i–n cell (b).

Table I. I_{sc}, V_{oc}, FF, and electric power for a-Si:H p–i–n cell with an area of $1.08\,\mathrm{cm}^2$, HIT-type cell with an area of $0.58\,\mathrm{cm}^2$, HIT-type cell with a filter of a-Si:H p–i–n, and multijunction cell constructed by stacking the a-Si:H p–i–n cell on the HIT type cell under illumination of AM 1.5 at $100\,\mathrm{mW/cm}^2$.

	I_{sc} (A)	V_{oc} (V)	FF	Power (mW)
a-Si:H p–i–n	1.23×10^{-2}	0.86	0.76	8.04
HIT	1.86×10^{-2}	0.58	0.75	8.35
HIT[a]	7.77×10^{-3}	0.56	0.78	3.39
Stacked cell	7.60×10^{-3}	1.34	0.61	6.21

a) a-Si:H p–i–n filtered

type cell so that I_{sc} and J_{sc} decreased to $7.77 \times 10^{-3}\,\mathrm{A}$ and $1.34 \times 10^{-2}\,\mathrm{A/cm}^2$, respectively, and V_{oc} slightly decreased to 0.56 V, as shown in Table I.

Figure 6 shows solar cell characteristics of a multijunction cell constructed by stacking the a-Si:H p–i–n cell on the HIT-type cell. AM 1.5 light was illuminated to the surface of the glass substrate of the a-Si:H p–i–n cell as shown in Fig. 5(a). Solar cell characteristics of each of the a-Si:H p–i–n cell, the HIT-type cell, and the HIT-type cell with an a-Si:H p–i–n cell filter are also presented in Fig. 6. A typical solar cell I–V curve was obtained for the stacked multijunction cell. A high V_{oc} of 1.34 V was observed. Although the reason why V_{oc} observed for the stacked cell was slightly lower than the sum of V_{oc}, 1.42 V, for the top a-Si:H p–i–n cell and the HIT-type cell with a filter of a-Si:H p–i–n cell is not clear yet, it means that the top and bottom solar cells
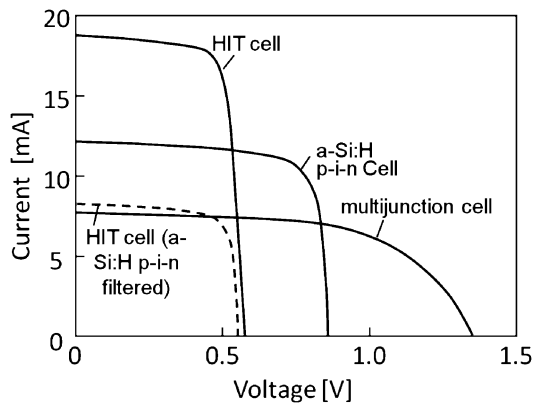
Fig. 6. Solar cell characteristics of a multijunction cell constructed by stacking the a-Si:H p–i–n cell on the HIT-type cell shown in Fig. 5(a). Solar cell characteristics of each of the a-Si:H p–i–n cell, the HIT-type cell, and the HIT-type cell with a filter of a-Si:H p–i–n are also presented.

simultaneously generated electric power. This clearly demonstrates that the present polyimide-ITO adhesive layer acted as a good optical and electrical connection between the two solar cells. The bottom HIT-type cell limited I_{sc} of the stacked cell because it had a small area and was not illuminated by a sufficient light intensity because of shading by the top cell. *FF* was low because of high R_c in the present demonstration. When J_{sc} of $1.31 \times 10^{-2}\,\mathrm{A/cm^2}$ ($= 7.6 \times 10^{-3}/0.58$) was used as at the bottom HIT-type cell, R_c was estimated to be $16\,\Omega\,\mathrm{cm^2}$ from eq. (1), for the stacked cell. Although R_c was high, the stacked cell generated a power of $6.21\,\mathrm{mW}$ under AM1.5 illumination, which was 1.83 times higher than that generated by the HIT-type cell under AM1.5 illumination with an a-Si:H p–i–n cell filter, as shown in Table I. The experimental results of Figs. 2 to 6 show a fundamental capability to fabricate multijunction solar cells by the mechanical stacking method using a polyimide transparent adhesive layer dispersed with ITO conductive particles.

4. Conclusions

A polyimide transparent adhesive layer dispersed with In_2O_3–SnO_2 (ITO) conductive particles was used for mechanical stacking of solar cells to fabricate multijunction solar cells. A 20-μm-thick polyimide-ITO layer had a high transmissivity in the range from 78 to 80% for wavelengths ranging from 500 to 1000 nm. This transparent characteristic is suitable to illuminating solar light onto an underlying bottom solar cell. The connecting resistivity of the polyimide-ITO layer is $2.3\,\Omega\,\mathrm{cm^2}$, at minimum, at the present stage. The low connecting resistivity is important to maintain high *FF* and conversion efficiency. A high V_{oc} of 1.34 V was experimentally demonstrated in the case of the multijunction solar cell by stacking the top a-Si:H p–i–n cell on the bottom HIT-type cell. Simultaneous electric power generation from the top and bottom solar cells was achieved. Those results showed the capability of fabricating multi-junction solar cells by mechanical stacking using a polyimide transparent adhesive layer dispersed with ITO conductive particles.

1) A. Rohatagi: Proc. 3rd World Conf. Photovoltaic Energy Conversion, 2003, p. A29.
2) M. A. Green: Prog. Photovoltaics **17** (2009) 183.
3) K. Yamamoto: Sol. Energy Mater. Sol. Cells **66** (2001) 117.
4) K. Nishioka, T. Takamori, T. Agui, M. Kaneiwai, Y. Uraoka, and T. Fuyuki: Jpn. J. Appl. Phys. **43** (2004) 882.
5) F. Meillaud, A. Shah, C. Droz, E. Vallat-Sauvain, and C. Miazza: Sol. Energy Mater. Sol. Cells **90** (2006) 2952.
6) S. P. Bremner, M. Y. Levy, and C. B. Honsberg: Prog. Photovoltaics **16** (2008) 225.
7) H. Sugiura, C. Amano, A. Yamamoto, and M. Yamaguchi: Jpn. J. Appl. Phys. **27** (1988) 269.
8) J. M. Olson, S. R. Kurtz, A. E. Kibbler, and P. Faine: Appl. Phys. Lett. **56** (1990) 623.
9) T. Takamoto, E. Ikeda, H. Kurita, M. Ohmori, M. Yamaguchi, and M. J. Yang: Jpn. J. Appl. Phys. **36** (1997) 6215.
10) M. Yamaguchi: Sol. Energy Mater. Sol. Cells **75** (2003) 261.
11) J. Takenezawa, M. Hasumi, T. Sameshima, T. Koida, T. Kaneko, M. Karasawa, and M. Kondo: Ext. Abstr. Solid State Devices and Materials, 2010, I-8-4.